International Journal of Design Engineering

ISSN online: 1751-5882 - ISSN print: 1751-5874
https://www.inderscience.com/ijde

Influence of steel fibres on the sorptivity of corroded reinforced concrete

Yuvraj Singh, Harvinder Singh

DOI: 10.1504/IJDE.2023.10054064

Article History:

Received:	05 May 2022
Last revised:	28 November 2022
Accepted:	30 December 2022
Published online:	05 July 2023

Influence of steel fibres on the sorptivity of corroded reinforced concrete

Yuvraj Singh*

I.K. Gujral Punjab Technical University,
Kapurthala, Punjab, India
and
Guru Nanak Dev Engineering College,
Ludhiana, Punjab, India
Email: uvraj_23@yahoo.co.in
*Corresponding author

Harvinder Singh

Guru Nanak Dev Engineering College,
Ludhiana, Punjab, India
Email: hvs1221@gmail.com

Abstract: The present paper describes the influence of steel fibres (SFs) on the sorptivity of RC members exposed to a corrosive environment. The concrete because of its inherent microstructure has a tendency to allow the ingress of moisture and other harmful gases into it, which triggers the corrosion of embedded rebars. The presence of other cracks therein further augments the rate of absorption that lead to their accelerated deterioration. With this background and the well-known crack-arresting potential of the SFs, an investigation was carried out on control, pre-loaded, and pre-corroded and loaded RC specimens to establish the effect of SFs in concrete on its rate of water absorption. In order to quantify this effect, sorptivity test was conducted on the cores extracted from the loaded un-corroded and corroded RC beams. It was found that inclusion of fibres alleviates the surface water absorption tendency of the concrete which enhances the durability.

Keywords: absorption; concrete; corrosion; durability; steel fibres; sorptivity.

Reference to this paper should be made as follows: Singh, Y. and Singh, H. (2023) 'Influence of steel fibres on the sorptivity of corroded reinforced concrete', *Int. J. Design Engineering*, Vol. 12, No. 1, pp.30–48.

Biographical notes: Yuvraj Singh is a PhD research scholar at I.K. Gujral Punjab Technical University, Kapurthala, India, and is currently an Assistant Professor in the Department of Civil Engineering, Guru Nanak Dev Engineering College, Ludhiana, India. He is engaged in teaching, research, and consultancy in structural engineering. His research interests include numerical modelling, structural health monitoring, durability of concrete structures and innovative materials in civil engineering.

Harvinder Singh is currently a Professor at Guru Nanak Dev Engineering College, Ludhiana, India. He is engaged in teaching, research, and consultancy in structural engineering. He has authored numerous technical publications, one laboratory manual, two monographs and has edited five books. He is UGC

Research Awardee, State Technical Auditor, Chartered Engineer and is a member of several professional bodies. He is an editorial board member and reviewer for several reputed Q1/Q2 international journals. His current research interests are mathematical modelling and limit analysis of engineering structures, largely directed towards solving practical problems and improving the related design practices.

1 Introduction

Due to the rapidly augmenting environmental concerns, it has become vital to use the resources judiciously and aim toward sustainability in every sphere including the construction industry. Concrete, being one of the most versatile and widely used construction materials, it becomes more important to do so. Concrete structures are sometimes exposed to extreme environments during their lifetime in addition to other service loading conditions. Any poor choice on part of either constituent materials, workmanship, or construction method often leads to a poor concrete microstructure, which further aggravates the problem in case of extreme environmental conditions. Therefore, the choice of construction material and construction methods for a specific application is a vital stage for eliminating durability issues. The concrete, being a quasi-brittle material is usually reinforced with steel rebars on the tension side of the members. Exposure to corrosive environments largely impacts the integrity of reinforced concrete (RC) as the concrete tends to crack in case of any overstress. Thus, it becomes crucial to ensure that the concrete should have low permeability throughout its service life. The use of steel fibres (SFs) has been well-researched in concrete for their superior crack-arresting potential and the improvement that it provides in its other properties (Alsayed and Alhozaimy, 1999; Thomas and Ramaswamy, 2007; El-Dieb, 2009; Afroughsabet and Ozbakkaloglu, 2015; Singh, 2015, 2016; Abbass et al., 2019; Wang and Kim, 2020; Abushanab et al., 2021; El-Hassan et al., 2021). Most of the documented research related to SFs in concrete emphasises on its capability to enhance the strength properties. In recent years, researchers have also investigated the effect of the inclusion of SFs in concrete on the durability properties of concrete (Ganesan et al., 2006; El-Dieb, 2009; Hubert et al., 2015; Ding et al., 2017a, 2017b, 2019a, 2019b; Ali et al., 2020; Fan et al., 2020; Abushanab et al., 2021; Kaplan et al., 2021; Singh et al., 2021; El Ouni et al., 2022). The reports related to the durability performance of the concrete containing SFs as documented in the literature are highly inconsistent.

Some of the researchers reported that the presence of SFs in concrete influences the durability properties including permeability negatively (El-Dieb, 2009; Mo et al., 2017; Ali et al., 2020; El Ouni et al., 2022; Wang et al., 2022). One of the reasons for the reported augmented water permeability could be either the presence of an excess of SFs or an improper technique of incorporation leading to balling effect. Therefore, when using SFs in concrete, it is vital to incorporate them skilfully and in appropriate proportions to get the maximum benefit out of them for strength and durability (Singh, 2017, 2021; Zhang et al., 2019).

Some of the researchers (El-Dieb, 2009; Abushanab et al., 2021; El Ouni et al., 2022) employed electrical techniques like rapid chloride penetration test (RCPT) to access the durability performance of concrete containing SFs. Such techniques involving the passing

of current through the test specimens are unsuitable for concrete containing conducting materials (Whiting and Mitchell, 1977; ASTM C1202, 2012; Bassuoni et al., 2006). The presence of metallic fibres or other conducting materials like admixtures provides an easy path for the flow of current resulting in misleading output. Furthermore, it has been clearly stated in the related standard that RCPT is not valid for concrete embedded with electrically conductive materials (ASTM C1202, 2012). Consequently, the results documented in the literature involving RCPT needs to be verified by using other suitable techniques that are recommended for the concrete containing conducting materials. Some of the applicable tests for assessing the durability properties of concrete containing metallic or conducting material are water permeability test, sorptivity test, bulk chloride diffusion test, colorimetric test, etc.

Some other studies involving the investigations on the permeability of test specimens reported that SFs play a significant role in reducing the crack permeability of concrete due to appreciable control on the crack propagation and crack widths (Li and Ding, 2017; Ding et al., 2018; Ding et al., 2019a; Li and Liu, 2020; Zeng and Ding, 2020; Zeng et al., 2020; Kaplan et al., 2021; Singh et al., 2021). Albeit, a huge inconsistency in results is found on reviewing the related literature, the evident crack-arresting potential of SFs strengthens the idea of a positive role that SFs can play in the concrete subjected to loading and exposed to a corrosive environment. Furthermore, the effect of the presence of SFs in concrete exposed to a corrosive environment on the 'sorptivity' has not been well researched. The corrosion of embedded rebars in RC interferes with its integrity, and hence, is bound to negatively affect its transport properties. Therefore, investigating the effect of the inclusion of SFs in such a concrete is crucial for wider applications. Keeping in view the well-known crack-arresting potential of SFs and the fact that they are metallic, it is vital to examine the transport property of concrete with SFs that is loaded as well as exposed to a corrosive environment. With this objective, an experimentation was designed involving the test specimens with and without SFs that were obtained from loaded un-corroded and corroded beams. The present paper records the beneficial effect of the fibre inclusion in the concrete in controlling its permeability and subsequently, the sorptivity which is a measure of the concrete's resistance to ingress of water or contaminants.

2 Experimental program

'Sorptivity test' as prescribed by ASTM C1589 was used to quantify the effect of SFs on the ingress of moisture into the concrete (ASTM C1585, 2007). SFs in concrete are well known to be crack arrestors. Therefore, in order to capture its effectiveness in doing so and further affect the rate of absorption of water, a set of pre-loaded and, pre-corroded and loaded test samples has been included in the experimental design. This section presents the details of the materials and specimens used in the investigations.

2.1 Materials

Ordinary portland cement (OPC) confirming to IS 8112 (BIS, 2013), fine aggregates and coarse aggregates conforming to IS 383 (BIS, 2016), and water was used in the making of concrete for the preparation of the test specimens. For steel fibre RC, hooked-end type

SFs having a 50 aspect ratio was used. The physical properties of the materials used are tabulated in Table 1.

Table 1 Physical properties of material used

Material	*Properties*	*Value*
Cement	Type	OPC
	Standard consistency	31%
	Initial setting time	39 min
	Final setting time	380 min
	Specific gravity	3.13
Fine aggregates	Type	Natural sand
	Specific gravity	2.64
	Fineness modulus	2.71
	Grading zone	II
Coarse aggregates	Type	Crushed stone
	Specific gravity	2.84
	Fineness modulus	6.8
	Maximum size	20 mm
Steel fibres	Thickness	1 mm
	Length	50 mm
	Aspect ratio	50
	Density	7,850 kg/m^3
	Shape	Hooked-end type

2.2 Mix proportions and preparation of test specimens

Plain cement concrete of grade M25 was proportioned as per IS 10262 (BIS, 2019); a concrete mix of 1: 1.4: 2.5 with a w/c ratio of 0.5 was found to give the target strength and workability. No deductions were made in the quantities of the aggregates in the case of steel fibre RC as the amount of fibres was small in comparison to the other constituents. The quantities of all ingredients of concrete are tabulated in Table 2.

Table 2 Quantities of ingredients of concrete

Constituents	*Quantity (Kg/m^3)*
Water	197.16
Cement	394.32
Fine aggregates	551.76
Coarse aggregates	968.44
Fibres	
0%	-
0.75%	58.87
1.5%	117.75

The concrete disks of 100±6 mm in diameter, with a specimen height of 50±3 mm, were prepared. To examine the influence of SFs on the sorptivity of concrete, the experimentation has been performed on nine sets, each consisting of three specimens, thereby making a total of 27 specimens. The specimens were categorised as follows depending on the exposure condition and each category consisted further of three different sets of specimens with varying percentages of SFs, i.e., 0%, 0.75%, and 1.5%:

a control specimens

b pre-loaded specimens

c pre-corroded and loaded specimens.

The control specimens are referred to as the standard un-loaded and un-corroded test samples. It consisted of a size 100±6 mm in diameter, with a length of 50±3 mm, and was obtained by core cutting from 150 mm × 150 mm × 150 mm concrete cubes (as illustrated in Figure 1) cast using 0%, 0.75%, and 1.5% of the SFs. All control test specimens were obtained after the concrete cubes were water-cured for 28 days. The obtained cores were later cut into the required lengths using the concrete cutter, the cross-sections of which are shown in Figure 2.

Figure 1 Core extraction from concrete cubes for control specimens (see online version for colours)

Figure 2 Typical core cross-sectional view of control specimens with (a) 0% SFs, (b) 0.75% SFs, (c) 1.5% SFs (see online version for colours)

(a) (b) (c)

The *pre-loaded specimens* are referred to as the test samples extracted from loaded RC beams. The samples of the required size were core cut from the pre-loaded RC concrete beams (as illustrated in Figure 3) cast using 0%, 0.75%, and 1.5% of the SFs. The obtained cores were later cut into the required lengths using the concrete cutter, the cross-sections of which are shown in Figure 4.

Figure 3 Core extraction from the tested RC beams for pre-loaded specimens (see online version for colours)

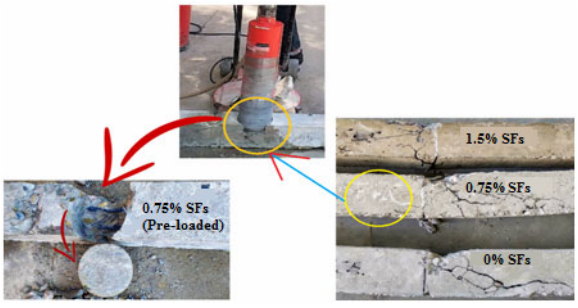

Figure 4 Typical core cross-sectional view of pre-loaded specimens with (a) 0% SFs, (b) 0.75% SFs, (c) 1.5% SFs (see online version for colours)

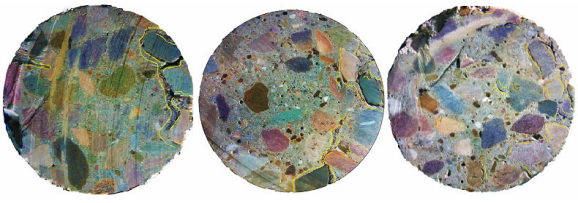

(a) (b) (c)

Corrosion of embedded rebars in concrete often leads to cracks due to the expansive nature of corrosion products and thus further deteriorates its durability due to the augmented rate of absorption. Therefore, to capture the role of SFs on the sorptivity of RC exposed to the corrosive environment, pre-corroded and loaded test samples have also been included in the experimental design.

The pre-corroded and loaded specimens were obtained from a set of RC beams, containing 0%, 0.75%, and 1.5% SFs, and subjected to an accelerated corrosion test for a period of one month, prior to the conduct of the bending test. A total of nine samples of the desired size were obtained by core cutting, as illustrated in Figure 5. The cross-sections of the pre-corroded and loaded test samples so obtained are shown in Figure 6.

Figure 5 Core extraction from the tested RC beams for pre-corroded and loaded specimens (see online version for colours)

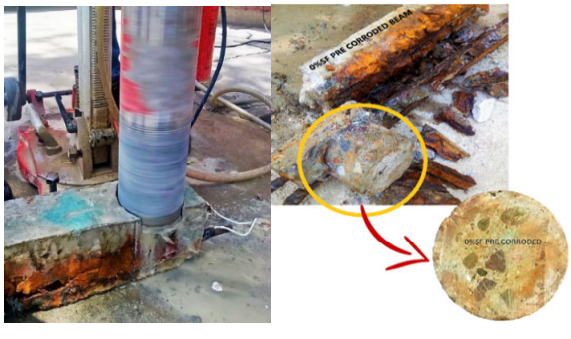

Figure 6 Typical core cross-sectional view of pre-corroded and loaded specimens with (a) 0% SFs, (b) 0.75% SFs, (c) 1.5% SFs (see online version for colours)

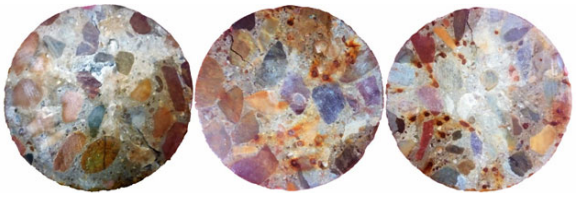

(a) (b) (c)

2.3 Testing

All the test samples were pre-conditioned as prescribed in the code (ASTM C1585, 2007). The diameter and mass of the samples were noted. Epoxy was used as a sealing material to seal the lateral surface of the specimens. One of the cross-sectional ends not to be exposed to water was covered using a plastic sheet to prevent any evaporation thereon. Following this, the mass of each of the sealed specimens was noted as the initial. The prepared samples were placed in the pan with the desired level of water above the support device as per the standard. The set-up as prescribed in the code (ASTM C1585, 2007) is illustrated in Figure 7. A pre-assigned water level was maintained throughout the test. The test samples were placed in position immediately after the onset of the stopwatch. The recordings post the beginning of the test was taken at different time intervals as prescribed in the code (Table 3). The prepared test set-up in the laboratory is shown in Figure 8. The absorption (I) in terms of 'mm' is calculated using equation (1), where ΔM_t = increment in the mass of sample (in grams), at the time t; A = exposed area of the sample (in mm^2), and ρ = density of water (in g/mm3);

$$I = \frac{\Delta M_t}{A \times \rho} \tag{1}$$

The initial rate of water absorption (in mm/s$^{1/2}$) is estimated from the slope of the line that is the best fit to the absorption (I) plotted against the square root of time (s$^{1/2}$). This slope is obtained using linear regression analysis by using points from 60 s to 6 h. The secondary rate of water absorption is obtained from the slope of the line that is the best fit of I plotted against the square root of time using all the points from 1 d to 7 d recording (ASTM C1585, 2007).

Figure 7 Set-up of the sorptivity test

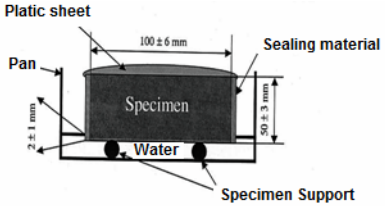

Source: ASTM C1585 (2007)

Figure 8 Prepared test set-up and specimens (see online version for colours)

Table 3 Time and tolerance for measurements schedule

Time	*60 s*	*5 min*	*10 min*	*20 min*	*30 min*	*60 min*	*Every hour up to 6 h*	*Once a day up to three days*	*Day 4 to 7* *Three measurements 24 h apart*	*Day 7 to 9* *One measurement*
Tolerance	2 s	10 s	2 min	2 min	2 min	2 min	5 min	2 h	2 h	2 h

Source: ASTM C1585 (2007)

3 Results and discussion

All the test specimens prepared as described in the previous section were tested identically using the procedure as prescribed in the code (ASTM C1585, 2007). The recordings of increments in the mass of the test samples were made at the intervals described in Table 3. Following this, the calculations were made to compute the sorptivity (I, *in* mm) which was measured as the ratio of increment in the mass of the test sample to the product of the exposed area of the cross-section of the sample and the density of water [*see equation (1)*]. The sorptivity test data for three different cases are listed in Tables 4 to 6.

The absorption vs. √time plot obtained from the sorptivity test data are shown in Figures 9 to 11.

From the sorptivity test data of the control test specimens, as tabulated in Table 4, the infiltration is found to be reduced by 33.59% and 52.52%, on the inclusion of 0.75% and 1.5% volume fraction of SFs, respectively, in the concrete in comparison to the specimens without SFs. In the absorption vs. √time plot, two distinct slopes are shown in each case of test specimens. The initial slope (from 60 s to 6 h) depicts the initial or early-age absorption, which was found to be steep, thereby indicating more infiltration during the initial periods of exposure to water in the sorptivity test. While the secondary slope represents the late-age absorption and the change in slope here indicates the saturation of the specimens. From the test results, the initial infiltration rate is found to be much higher in the case of cement concrete without SFs in comparison to the specimens

with 0.75% and 1.5% SFs. From the linear regression analysis, and as illustrated in Figure 9, the initial infiltration rate of the control specimens is found to be lowered on the inclusion of 0.75% and 1.5% SFs by 29.88% and 50.46%, respectively, in comparison to the control concrete specimens without SFs. This decline in the rate of infiltration in the specimens containing SFs is accounted to the augmented time lag provided by SFs by acting as a barrier to the flow of water. Furthermore, being a crack arrestor, the presence of SFs also tends to eliminate the micro-cracks in the concrete that may originate due to shrinkage. The secondary rate of absorption remained significantly lower than the initial rate of absorption for all cases. Thus, the lowered rate of absorption on the inclusion of SFs to concrete gives evidence of improved durability of the concrete due to decreased rate of ingress of water.

Figure 9 Absorption vs. √time plot of the control test specimens (see online version for colours)

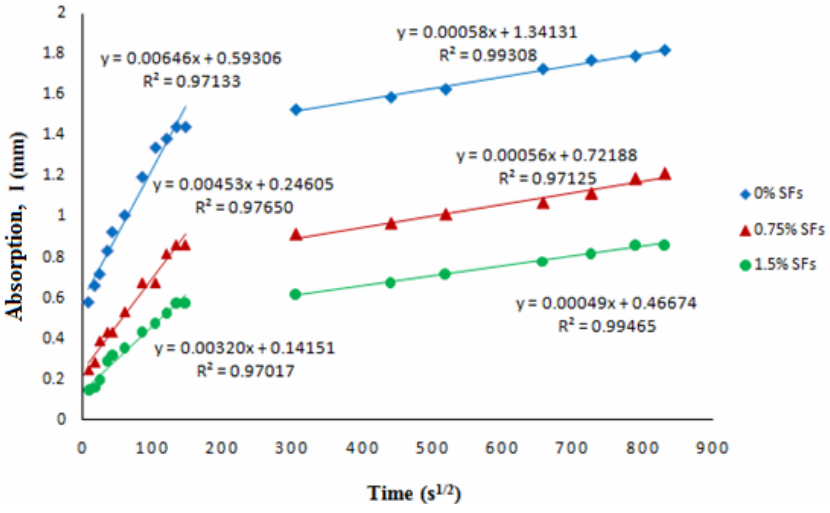

Table 5 shows the test data of the pre-loaded test specimens. The absorption, in this case, is evidently higher than the control case for all sets of specimens due to the introduction of structural cracks in the pre-loaded specimens. It has been observed that in the case of the pre-loaded test specimens, sorptivity lowered on the inclusion of 0.75% and 1.5% SFs in concrete by 19.91% and 37.91%, respectively, in comparison to the pre-loaded concrete specimens without any SFs. From the test results of pre-loaded test specimens, the initial infiltration rate is again found to be higher in the case of cement concrete without SFs in comparison to the specimens with 0.75% and 1.5% SFs. From the linear regression analysis, and as illustrated in Figure 10, the initial infiltration rate of the pre-loaded specimens is found to be lowered on the inclusion of 0.75% and 1.5% SFs by 9.06% and 27.39%, respectively, in comparison to the pre-loaded concrete specimens without any SFs. This decline in the absorption and sorptivity is accounted to the presence of SFs which act as crack arresters and thus reduce the cracks to a greater extent in the case of pre-loaded specimens. In the case of pre-loaded specimens too, the secondary rate of infiltration remained considerably less than the initial rate of absorption for all cases. Thus, reduced cracks result in lower infiltration of water and hence enhanced durability of concrete.

Table 4 Sorptivity test data of the control specimens

Test time (sec)	*Time* ($s^{1/2}$)	*Mass of sample, M (grams)*			*Increment in mass, ΔM (grams)*			*Increment in mass/area/water density, I (mm)*		
		0% SFs	*0.75% SFs*	*1.5% SFs*	*0% SFs*	*0.75% SFs*	*1.5% SFs*	*0% SFs*	*0.75% SFs*	*1.5% SFs*
0	0	781.0	824.6	833.3	0	0	0	0	0	0
60	8	784.6	826.3	834.3	4.0	1.7	1.0	0.582	0.245	0.144
300	17	785.6	826.3	834.3	4.6	2.0	1.1	0.663	0.283	0.156
600	24	786.0	827.3	834.3	5.0	2.7	1.3	0.720	0.389	0.194
1,200	35	786.0	827.6	835.3	5.8	3.0	2.0	0.834	0.432	0.288
1,800	42	788.0	827.6	835.6	6.4	3.0	2.2	0.926	0.432	0.319
3,600	60	788.0	828.3	836.0	7.0	3.7	2.4	1.008	0.533	0.352
7,200	85	789.3	829.3	836.3	8.3	4.7	3.0	1.196	0.677	0.432
10,800	104	790.3	829.3	836.6	9.3	4.7	3.3	1.340	0.677	0.476
14,400	120	790.6	830.3	836.6	9.6	5.7	3.6	1.383	0.821	0.523
18,000	134	791.0	830.6	837.3	10.0	6.0	4.0	1.441	0.865	0.576
21,600	147	791.0	830.6	837.3	10.0	6.0	4.0	1.441	0.865	0.576
92,220	304	791.6	831.3	837.6	10.6	6.3	4.3	1.527	0.911	0.619
193,200	440	792.3	831.3	838.0	11.0	6.7	4.7	1.588	0.965	0.677
268,500	518	792.3	831.6	838.3	11.3	7.0	5.0	1.628	1.009	0.720
432,000	657	793.0	832.0	838.3	12.0	7.4	5.4	1.729	1.066	0.782
527,580	726	793.3	833.0	839.0	12.3	7.7	5.7	1.772	1.112	0.821
622,200	789	793.3	833.0	839.3	12.4	8.2	6.0	1.792	1.185	0.865
691,200	831	794.3	833.3	839.3	12.6	8.4	6.0	1.822	1.210	0.865

Table 5 Sorptivity test data on the pre-loaded specimens

Test time (sec)	*Time* ($s^{1/2}$)	*Mass of sample, M (grams)*			*Increment in mass, ΔM (grams)*			*Increment in mass/area/water density, I (mm)*		
		0% SFs	*0.75% SFs*	*1.5% SFs*	*0% SFs*	*0.75% SFs*	*1.5% SFs*	*0% SFs*	*0.75% SFs*	*1.5% SFs*
0	0	754.3	817.6	829.0	0	0	0	0	0	0
60	8	757.3	819.3	830.3	3.0	1.7	1.3	0.432	0.245	0.187
300	17	758.6	820.3	831.0	4.3	2.7	2.0	0.619	0.389	0.288
600	24	759.3	821.6	831.6	5.0	4.0	2.6	0.72	0.576	0.375
1,200	35	760.3	822.0	832.3	6.0	4.4	3.3	0.865	0.634	0.475
1,800	42	762.0	823.3	833.3	6.6	5.7	4.3	0.952	0.821	0.619
3,600	60	762.3	824.6	834.0	7.8	6.3	5.0	1.124	0.915	0.720
7,200	85	764.0	825.0	834.6	9.8	7.4	5.6	1.415	1.066	0.807
10,800	104	764.6	826.0	835.6	10.6	8.4	6.6	1.532	1.210	0.951
14,400	120	765.6	827.0	836.3	11.3	9.4	7.3	1.625	1.354	1.052
18,000	134	767.3	828.0	837.0	11.9	10.2	8.0	1.715	1.473	1.152
21,600	147	768.0	829.0	837.6	13.0	11.0	8.4	1.873	1.585	1.215
92,220	304	769.6	830.0	838.3	15.3	12.4	9.3	2.205	1.787	1.340
193,200	440	771.0	831.0	839.3	16.7	13.4	10.3	2.406	1.931	1.484
268,500	518	771.3	831.3	839.6	17.0	13.7	10.6	2.449	1.974	1.527
432,000	657	772.6	832.3	840.6	18.3	14.7	11.6	2.636	2.118	1.671
527,580	726	773.6	833.0	841.6	19.3	15.4	12.0	2.781	2.219	1.725
622,200	789	774.6	834.0	842.0	20.3	16.1	12.6	2.925	2.315	1.816
691,200	831	755.0	834.6	842.6	20.7	16.6	12.8	2.983	2.389	1.852

Table 6 Sorptivity test data on the pre-corroded and loaded specimens

Test time (sec)	*Time* $(s^{1/2})$	*Mass of sample, M (grams)*			*Increment in mass,* ΔM *(grams)*			*Increment in mass/area/water density, I (mm)*		
		0% SFs	*0.75% SFs*	*1.5% SFs*	*0% SFs*	*0.75% SFs*	*1.5% SFs*	*0% SFs*	*0.75% SFs*	*1.5% SFs*
0	0	748.0	780.6	795.0	0	0	0	0	0	0
60	8	750.3	782.3	796.0	2.3	1.7	1.0	0.331	0.245	0.144
300	17	751.6	783.6	796.3	3.6	3.0	1.4	0.519	0.432	0.205
600	24	752.3	784.3	797.6	4.6	3.7	2.6	0.663	0.533	0.375
1,200	35	753.0	785.6	798.3	5.0	5.0	3.3	0.720	0.720	0.475
1,800	42	754.6	787.0	799.0	6.6	5.7	4.0	0.951	0.815	0.576
3,600	60	755.3	787.3	800.6	7.3	6.7	5.0	1.052	0.965	0.715
7,200	85	756.6	788.6	802.0	9.2	7.7	5.7	1.325	1.115	0.823
10,800	104	758.3	789.0	802.3	10.3	8.9	7.0	1.484	1.285	1.008
14,400	120	759.6	789.6	803.6	11.6	9.4	7.7	1.671	1.354	1.115
18,000	134	760.3	791.0	804.6	13.0	10.4	8.4	1.874	1.498	1.205
21,600	147	762.6	791.3	805.3	14.6	11.3	9.2	2.104	1.635	1.325
92,220	304	763.3	792.6	805.6	15.3	12.0	10.6	2.205	1.729	1.527
193,200	440	764.6	793.3	806.3	16.6	13.0	11.3	2.392	1.875	1.628
268,500	518	765.3	794.6	807.6	17.3	14.0	12.0	2.493	2.017	1.735
432,000	657	766.0	795.3	808.3	18.7	15.0	13.3	2.695	2.158	1.916
527,580	726	767.3	796.3	809.0	19.3	15.7	14.0	2.781	2.262	2.017
622,200	789	768.6	797.6	810.3	20.6	16.1	14.3	2.968	2.325	2.058
691,200	831	769.0	798.6	810.6	21.0	16.6	14.6	3.026	2.395	2.105

Figure 10 Absorption vs. √time plot of the pre-loaded test specimens (see online version for colours)

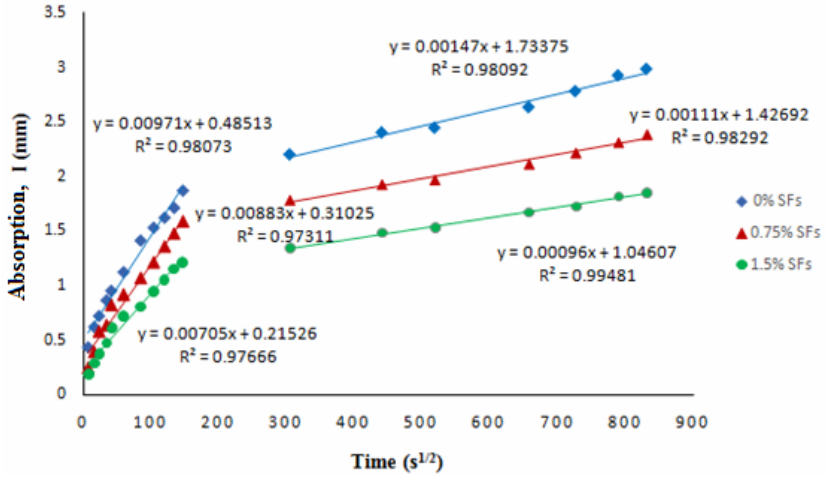

Figure 11 Absorption vs. √time plot of the pre-corroded and loaded test specimens (see online version for colours)

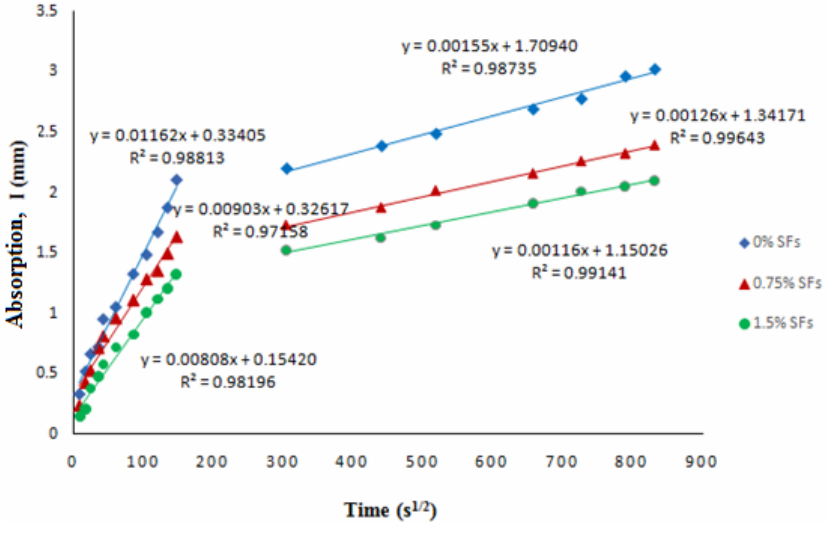

Table 6 shows the test data of the pre-corroded and loaded test specimens. The absorption, in this case, is found to be higher than both the control case and the pre-loaded case as well. This is because of the deterioration caused due to both pre-loading as well as the corrosion of the RC beams from which the samples under consideration were obtained. It has been observed that in the case of the pre-corroded and loaded test specimens, sorptivity lowered on the inclusion of 0.75% and 1.5% SFs in concrete by 20.85% and 30.44%, respectively, in comparison to the pre-corroded and loaded concrete specimens without any SFs. Furthermore, the initial infiltration rate is again found to be higher in the case of cement concrete without SFs in comparison to the

specimens with 0.75% and 1.5% SFs. From the linear regression analysis, and as illustrated in Figure 11, the initial infiltration rate of the pre-corroded and loaded specimens is found to be lowered on the inclusion of 0.75% and 1.5% SFs by 22.29% and 30.46%, respectively, in comparison to the pre-corroded and loaded concrete specimens without any SFs. The secondary absorption rate remained significantly lower than the initial rate of absorption for all cases. This decline in the rate of infiltration in the pre-corroded and loaded test specimens containing SFs is due to the crack-arresting potential of SFs. Furthermore, the SFs acted as sacrificial anodes which helped in reducing rebar corrosion and hence reduced cracks that may arise due to corrosion of rebars. Thus, reduced cracks resulted in lower infiltration of water and hence the improved durability of the concrete when exposed to corrosive environments also. Table 7 shows the summary of the initial and secondary rate of absorption in each set of specimens.

Table 7 Summary of sorptivity in each set of test specimen

Type	*Control specimen*			*Pre-loaded specimen*			*Pre-corroded and loaded specimen*		
	0% SFs	*0.75% SFs*	*1.5% SFs*	*0% SFs*	*0.75% SFs*	*1.5% SFs*	*0% SFs*	*0.75% SFs*	*1.5% SFs*
Initial rate of absorption ($\times 10^{-3}$ mm/$\sqrt{s}$)	6.46	4.53	3.20	9.71	8.83	7.05	11.62	9.03	8.08
Secondary rate of absorption ($\times 10^{-3}$ mm/$\sqrt{s}$)	0.58	0.56	0.49	1.47	1.11	0.96	1.55	1.26	1.16

Table 8 Percentage of surface water on the specimens after the sorptivity test

Steel fibre content	*Surface water percentage (%) of the specimens after the sorptivity test*					
	Control specimens		*Pre-loaded specimens*		*Pre-corroded and loaded specimens*	
	Surface water %	*Average*	*Surface water %*	*Average*	*Surface water %*	*Average*
0% SFs	26.75	28.39	40.18	42.79	46.19	47.88
	28.25		42.65		47.27	
	30.17		45.54		50.19	
0.75% SFs	18.69	20.99	33.56	35.80	32.49	36.96
	21.77		35.12		38.18	
	22.53		38.73		40.21	
1.5% SFs	13.78	15.43	20.40	23.89	26.74	28.42
	15.19		25.13		28.15	
	17.33		26.14		30.38	

After the determination of the rate of absorption in each set of specimens subjected to the sorptivity test, the surface water percentage of specimens was worked out by image

processing as illustrated in Figures 12 to 14. The results so obtained are summarised in Table 8.

Figure 12 Surface water percentage of standard control sample with (a) 0% SFs, (b) 0.75% SFs, (c) 1.5% SFs (see online version for colours)

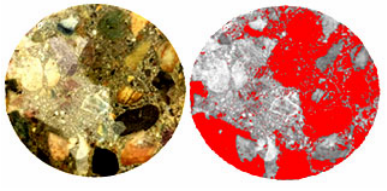

(a)

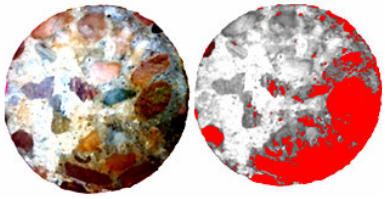

(b)

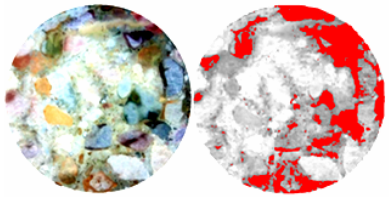

(c)

Figure 13 Surface water percentages of pre-loaded samples with (a) 0% SFs, (b) 0.75% SFs, (c) 1.5% SFs (see online version for colours)

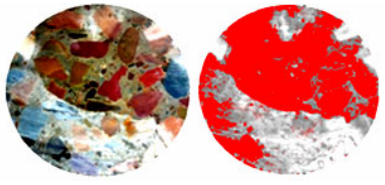

(a)

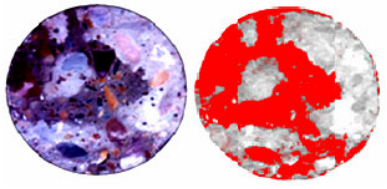

(b)

Figure 13 Surface water percentages of pre-loaded samples with (a) 0% SFs, (b) 0.75% SFs, (c) 1.5% SFs (continued) (see online version for colours)

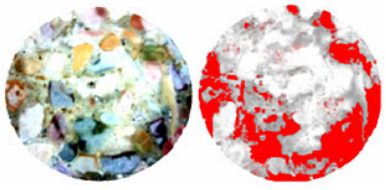

(c)

Figure 14 Surface water percentages of pre-loaded and corroded samples with (a) 0% SFs, (b) 0.75% SFs, (c) 1.5% SFs (see online version for colours)

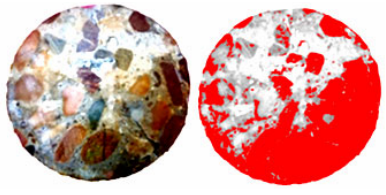

(a)

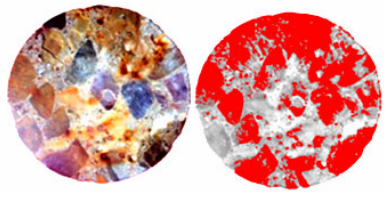

(b)

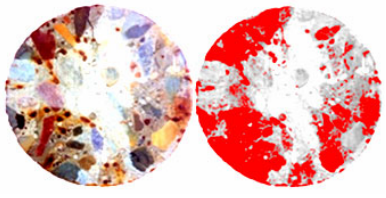

(c)

Post the sorptivity test, the percentage of surface water is found to be greater in the case of the standard concrete specimens without any SFs in comparison to that of steel fibre RC specimens for all sets of specimens. Furthermore, the percentage of surface water is found to be higher in the pre-loaded specimens and is highest in the case of the pre-corroded and the loaded specimens as compared to the control specimens. This is due to the cracks arising due to loading in the case of the pre-loaded specimens and cracks due to loading and corrosion of the rebars in the case of the pre-corroded and the loaded specimens. In the case of the control specimens, the reduced sorptivity and hence the reduced surface water percentage in the case of the specimens with the SFs is accounted to the reduced shrinkage cracks and the time lag provided by the fibres. Furthermore, in the case of the pre-loaded specimens and the pre-corroded and loaded specimens, the SFs

play a vital role in arresting the cracks, both due to the loading as well as the ones arising due to corrosion of the rebars. Thus, SFs aid in reducing the ingress of water resulting in reduced surface water percentage and hence leading to enhanced durability of the concrete.

4 Conclusions

The primary conclusions drawn from this experimental investigation are listed below:

- The sorptivity in the case of the concrete specimen containing SFs is found to be less than the plain cement concrete specimens.
- The sorptivity is observed to be higher in the case of the pre-loaded specimens as compared to the control ones. When compared to the conventional concrete pre-loaded specimens, the specimens containing SFs showed a reduced rate of absorption.
- The sorptivity is found to be further accelerated in the pre-corroded and the loaded specimen in comparison to the pre-loaded and the standard specimens. When compared to conventional concrete pre-corroded and loaded specimens, the specimens containing SFs showed a significantly reduced rate of absorption and this is accounted to the crack-arresting potential of the SFs and reduced distress due to the corrosive environment.
- The surface water percentage is found to be proportional to the rate of absorption of specimens. Consequently, it is found to be higher in pre-loaded and pre-corroded and loaded specimens as compared to control specimens, due to increased sorptivity. Furthermore, surface water percentage is observed to be reduced in the case of specimens with SFs due to decreased infiltration.

Acknowledgements

The authors would like to express their heartiest appreciation and acknowledgement for all those at Guru Nanak Dev. Engineering College, Ludhiana, and I.K. Gujral Punjab Technical University, Kapurthala, who rendered help and support in this research project.

References

Abbass, A., Abid, S. and Özakça, M. (2019) 'Experimental investigation on the effect of steel fibers on the flexural behavior and ductility of high-strength concrete hollow beams', *Advances in Civil Engineering*, DOI: 10.1155/2019/8390345.

Abushanab, A. et al. (2021) 'Mechanical and durability properties of ultra-high performance steel FRC made with discarded materials', *Journal of Building Engineering*, Vol. 44, DOI: 10.1016/j.jobe.2021.103264.

Afroughsabet, V. and Ozbakkaloglu, T. (2015) 'Mechanical and durability properties of high-strength concrete containing steel and polypropylene fibers', *Construction and Building Materials*, Vol. 94, pp.73–82, DOI: 10.1016/j.conbuildmat.2015.06.051.

Ali, B. et al. (2020) 'Effect of varying steel fiber content on strength and permeability characteristics of high strength concrete with micro silica', *Materials*, Vol. 13, No. 24, pp.1–17. doi: 10.3390/ma13245739.

Alsayed, S.H. and Alhozaimy, A.M. (1999) 'Ductility of concrete beams reinforced with FRP bars and steel fibers', *Journal of Composite Materials*, Vol. 33, No. 19, pp.1792–1806, DOI: 10.1177/002199839903301902.

ASTM C1202 (2012) *Standard Test Method for Electrical Indication of Concrete's Ability to Resist Chloride*, No. 12, pp.1–8, DOI: 10.1520/C1202-12.2.

ASTM C1585 (2007) *Standard Test Method for Measurement of Rate of Absorption of Water by Hydraulic-Cement Concretes ASTM C 1585:2007*, American Society for Testing and Materials., pp. 1–6.

Bassuoni, M.T., Nehdi, M.L. and Greenough, T.R. (2006) 'Enhancing the reliability of evaluating chloride ingress in concrete using the ASTM C 1202 rapid chloride penetrability test', *Journal of ASTM International*, Vol. 3, No. 3, DOI: 0.1520/jai13403.

BIS (2013) *IS 8112: Indian Standard Ordinary Portland cement, 43 grade–specification*, Bureau of Indian Standards: New Delhi, India, 2013: Bureau of Indian Standards: New Delhi, India.

BIS (2016) *IS 383: Specification for Coarse and Fine Aggregates From Natural Sources for Concrete*, Bureau of Indian Standards: New Delhi, India.

BIS (2019) *IS 10262: Concrete Mix Proportioning – Guidelines*, Bureau of Indian Standards, New Delhi, India.

Ding, Y., Li, D. and Zhang, Y. (2018) 'Quantitative analysis of macro steel fiber influence on crack geometry and water permeability of concrete', *Composite Structures*, Vol. 187, pp.325–335, DOI: 10.1016/j.compstruct.2017.12.074.

Ding, Y., Ren, X. and Li, D. (2017a) 'Investigation of the fiber effect on the permeability of cracked concrete', *Shuili Xuebao/Journal of Hydraulic Engineering*, Vol. 48, No. 1, pp.13–20, DOI: 10.13243/j.cnki.slxb.20160332.

Ding, Y., Wang, Q. and Lin, Y. (2017b) 'Effect of fibers on permeability and crack relaxation of cracked concrete', *Fuhe Cailiao Xuebao/Acta Materiae Compositae Sinica*, Vol. 34, No. 8, pp.1853–1861, DOI: 10.13801/j.cnki.fhclxb.20161202.002.

Ding, Y., Hao, X. and Men, X. (2019a) 'Effect of fiber on the crack width, tortuosity and permeability of concrete | 纤维对混凝土裂缝宽度, 曲折度及渗透性的影响', *Fuhe Cailiao Xuebao/Acta Materiae Compositae Sinica*, Vol. 36, No. 2, pp.491–497, DOI: 10.13801/j.cnki.fhclxb.20180413.004.

Ding, Y., Zhu, H. and Li, D. (2019b) 'Effect of macro steel fiber on permeability and damage of concrete under uniaxial compression | 结构型钢纤维对单轴受压下混凝土渗透性及损伤的影响', *Fuhe Cailiao Xuebao/Acta Materiae Compositae Sinica*, Vol. 36, No. 12, pp.2942–2949, DOI: 10.13801/j.cnki.fhclxb.20190314.004.

El-Dieb, A.S. (2009) 'Mechanical, durability and microstructural characteristics of ultra-high-strength self-compacting concrete incorporating steel fibers', *Materials and Design*, Vol. 30, No. 10, pp.4286–4292, DOI: 10.1016/j.matdes.2009.04.024.

El-Hassan, H. et al. (2021) 'Performance of steel fiber-reinforced alkali-activated slag-fly ash blended concrete incorporating recycled concrete aggregates and dune sand', *Buildings*, Vol. 11, No. 8, DOI: 10.3390/buildings11080327.

El Ouni, M.H. et al. (2022) 'Mechanical performance, water and chloride permeability of hybrid steel-polypropylene fiber-reinforced recycled aggregate concrete', *Case Studies in Construction Materials*, Vol. 16, DOI: 10.1016/j.cscm.2021.e00831.

Fan, L. et al. (2020) 'Effects of lightweight sand and steel fiber contents on the corrosion performance of steel rebar embedded in UHPC', *Construction and Building Materials*, Vol. 238, DOI: 10.1016/j.conbuildmat.2019.117709.

Ganesan, N., Indira, P.V and Kumar, P.T.S. (2006) 'Durability aspects of steel fibre-reinforced SCC', *Indian Concrete Journal*, Vol. 80, No. 5, pp.31–37.

Hubert, M., Desmettre, C. and Charron, J-P. (2015) 'Influence of fiber content and reinforcement ratio on the water permeability of reinforced concrete', *Materials and Structures/Materiaux et Constructions*, Vol. 48, No. 9, pp.2795–2807, DOI: 10.1617/s11527-014-0354-z.

Kaplan, G. et al. (2021) 'Mechanical and durability properties of steel fiber-reinforced concrete containing coarse recycled concrete aggregate', *Structural Concrete*, Vol. 22, No. 5, pp.2791–2812, DOI: 10.1002/suco.202100028.

Li, D. and Ding, Y. (2017) 'Effects of macro fibers on the permeability of cracked concrete', *Tumu Gongcheng Xuebao/China Civil Engineering Journal*, Vol. 50, No. 10, pp.62–68.

Li, D. and Liu, S. (2020) 'The influence of steel fiber on water permeability of concrete under sustained compressive load', *Construction and Building Materials*, Vol. 242, DOI: 10.1016/j.conbuildmat.2020.118058.

Mo, K.H. et al. (2017) 'Mechanical, toughness, bond and durability-related properties of lightweight concrete reinforced with steel fibres', *Materials and Structures/Materiaux et Constructions*, Vol. 50, No. 1, DOI: 10.1617/s11527-016-0934-1.

Singh, H. (2015) 'Steel fibers as the only reinforcement in concrete slabs: flexural response and design chart', *Structural Engineering International: Journal of the International Association for Bridge and Structural Engineering (IABSE)*, Vol. 25, No. 4, pp.432–441, DOI: 10.2749/101686615X14355644771090.

Singh, H. (2016) 'Flexural modelling of steel-fibre-reinforced concrete member with conventional tensile rebars', *Proceedings of the Institution of Civil Engineers: Structures and Buildings*, Vol. 169, No. 1, pp.54–66, DOI: 10.1680/stbu.14.00054.

Singh, H. (2017) 'Steel fiber reinforced concrete: behavior, modelling and design', *Springer Transactions in Civil and Environmental Engineering*, Springer, Singapore, DOI: 10.1007/978-981-10-2507-5.

Singh, H. (2021) 'Structural Materials: behavior, testing and evaluation', *Materials Horizons: from Nature to Nanomaterials*, Springer, Singapore, DOI: 10.1007/978-981-16-3211-2.

Singh, Y., Singh, S. and Singh, H. (2021) 'Effect of steel fibers on the sorptivity of concrete', in Seetharamu, S., Jagadish, T. and Malagi, R.R. (Eds.): *Fatigue, Durability, and Fracture Mechanics. Lecture Notes in Mechanical Engineering*, pp.479–492, Springer, Singapore, DOI: 10.1007/978-981-15-4779-9_32.

Thomas, J. and Ramaswamy, A. (2007) 'Mechanical properties of steel fibre-reinforced concrete', *Journal of Materials in Civil Engineering*, Vol. 19, No. 5, pp.385–392, DOI: 10.1061/_ASCE0899-1561_200719:5_385.

Wang, J. and Kim, Y.J. (2020) 'Functional characteristics of ultra-high-performance concrete comprising various fibers', *ACI Materials Journal*, Vol. 117, No. 5, pp.179–191, DOI: 10.14359/51725978.

Wang, Y. et al. (2022) 'Quantitative evaluation of the characteristics of air voids and their relationship with the permeability and salt freeze-thaw resistance of hybrid steel-polypropylene fiber-reinforced concrete composites', *Cement and Concrete Composites*, Vol. 125, DOI: 10.1016/j.cemconcomp.2021.104292.

Whiting, D. and Mitchell, T.M. (1977) *History of the Rapid Chloride Permeability Test*, No. 16, pp.55–62.

Zeng, W. and Ding, Y. (2020) 'Effects of macro fibers on crack permeability evolution of concrete under loading | 荷载作用下结构型纤维对混凝土裂缝渗透率演化的影响', *Fuhe Cailiao Xuebao/Acta Materiae Compositae Sinica*, Vol. 37, No. 9, pp.2314–2323, DOI: 10.13801/j.cnki.fhclxb.20191213.001.

Zeng, W. et al. (2020) 'Effect of steel fiber on the crack permeability evolution and crack surface topography of concrete subjected to freeze-thaw damage', *Cement and Concrete Research*, Vol. 138, DOI: 10.1016/j.cemconres.2020.106230.

Zhang, P. et al. (2019) 'Durability of steel fiber-reinforced concrete containing SiO2 nano-particles', *Materials*, Vol. 12, No. 13, DOI: 10.3390/ma12132184.